A QUANTUM MECHANICAL CALCULATION OF THE RADIAL DISTRIBUTION FUNCTION FOR A PLASMA

By A. A. Barker*

[*Manuscript received December* 22, 1967]

Summary

A quantum mechanical calculation of the radial distribution function $g_{\text{q.m.}}(r)$ for unlike particles in a hydrogenous plasma is presented. Results for a neutral plasma over a range of temperatures show that $g_{\text{q.m.}}(r)$ differs significantly from the corresponding classical distribution function $g_{\text{c}}(r) = \exp(\beta e^2/r)$ when r is less than a chosen distance r_j, the value of which is temperature dependent. The effect of shielding, the relative contribution from scattered and bound states, and the relation to percentage ionization are discussed.

I. Introduction

In solving a modified Percus–Yevick integral equation for a hydrogenous plasma to find the radial distribution function for unlike particles for temperatures near 10^4 °K, it was found (Barker 1966) that the efficiency of the numerical iterative procedure used was very sensitive to the initial form assumed for the radial distribution function. If a classical or Debye–Hückel form was used, the cutoff point as r became small was of critical importance to the solution. This reflects the fact that at these temperatures an appreciable number of particles of opposite charges are bound, and the classical theory does not adequately describe the bound states. To overcome this difficulty a quantum mechanical expression for the radial distribution function at low radii has been evaluated, the results of which are presented in this paper.

II. Quantum Mechanical Expression for $g_{ab}(r)$

The radial distribution function $g_{ab}(r)$ is usually defined by $D_{ab}(r) = D_b g_{ab}(r)$, where $D_{ab}(r)$ is the number density of particles of type b at a distance r from a particle of type a, and D_b is the average number density of type b particles throughout the fluid. It is proportional to the conditional probability of finding particle b in volume element $\mathrm{d}x(2)$ given particle a in volume element $\mathrm{d}x(1)$, and, for a neutral plasma of electron number density D_{e}, the distribution function between protons and electrons can be expressed as

$$g_{\text{q.m.}}(r) = \frac{\sum\limits_{n} \exp(-\beta E_n)\,\psi_{nlm}\psi^*_{nlm} + \sum\limits_{\mathbf{k}} \exp(-\beta \mathbf{k}^2\hbar^2/2m)\,\psi_{\mathbf{k}}\psi^*_{\mathbf{k}}}{\sum\limits_{\mathbf{k}} \exp(-\beta \mathbf{k}^2\hbar^2/2m)\,\psi_0\psi^*_0}, \tag{1}$$

where the summation over n sums over the bound states of energy E_n of the hydrogen atom, and ψ_{nlm} are the wavefunctions normalized so that $\int \psi_{nlm}\psi^*_{nlm}\,\mathrm{d}V = 1$. The

* Department of Mathematical Physics, University of Adelaide, S.A. 5000.

summation over **k** sums over scattered states of the hydrogen atom and $\psi_{\mathbf{k}}$ are the wavefunctions normalized so that $\int \psi_{\mathbf{k}} \psi_{\mathbf{k}}^* \, \mathrm{d}V = 1$. ψ_0 is the wavefunction of an electron without a proton present, that is, a plane wave, but normalized so that $\int \psi_0 \psi_0^* \, \mathrm{d}V = 1$. Substituting the wavefunctions as given by Pauling and Wilson (1935) and Schiff (1955), replacing the summation over **k** by an integral, and removing the angular dependence, we have

$$g_{\mathrm{q.m.}}(r) = \Big\{ \sum_{n=1}^{\infty} \exp(-\beta E_n) \sum_{l=0}^{n-1} \frac{2l+1}{4\pi} \left(\frac{2Z}{na_0}\right)^3 \frac{(n-l-1)!}{2n\{(n+l)!\}^3} \exp(-\rho)\, \rho^{2l} \{\mathrm{L}_{n+l}^{2l+1}(\rho)\}^2 + \frac{2}{(2\pi)^2} \int_0^{\infty} \exp(-\beta k^2 \hbar^2/2m) \sum_{l=0}^{\infty} \frac{2l+1}{k^2 r^2} \{\mathrm{F}_l(\alpha, kr)\}^2 \, k^2 \, \mathrm{d}k \Big\} \div \frac{4\pi}{(2\pi)^3} \int_0^{\infty} \exp(-\beta k^2 \hbar^2/2m) \, k^2 \, \mathrm{d}k . \tag{2}$$

where $\rho = 2rZ/na_0$ (a_0 being the first Bohr radius, Z the atomic number, and n the principal quantum number), L_{n+l}^{2l+1} are the associated Laguerre polynomials, and $\mathrm{F}_l(\alpha, kr)$ are the Coulomb wavefunctions with $\alpha = Zme^2/\hbar^2 k$. Evaluating the denominator directly gives $(2\pi\beta\hbar^2/m)^{-3/2}$ cm^{-3}, which can be conveniently expressed in units of (Bohr radii)$^{-3}$, and we have

$$g_{\mathrm{q.m.}}(r) = \left(\frac{2\pi\beta\hbar^2}{m}\right)^{3/2} \Big\{ \frac{Z^3}{\pi} \sum_{n=1}^{\infty} \frac{\exp(-\beta E_n - \rho)}{n^4} \sum_{l=0}^{n-1} \frac{(2l+1)(n+l+1)!}{\{(n+l)!\}^3} \, \rho^{2l} \{\mathrm{L}_{n+l}^{2l+1}(\rho)\}^2 + \frac{1}{2\pi^2 r^2} \int_0^{\infty} \exp(-\beta k^2 \hbar^2/2m) \sum_{l=0}^{\infty} (2l+1) \{\mathrm{F}_l(\alpha, kr)\}^2 \, \mathrm{d}k \Big\} . \tag{3}$$

III. Evaluation of $g_{\mathrm{q.m.}}(r)$ and Results

The associated Laguerre polynomials were generated by two methods, one using recurrence relations and the other using a power series, so providing a consistency check. The zero and first-order Coulomb functions were similarly generated by two methods, one using a power series and the other using an asymptotic expansion, depending on the range of α and ρ; the recurrence relation technique of Abramowitz and Stegun (1964) was then used to generate the functions of higher order. A computer programme was written for a C.D.C. 6400 computer to evaluate $g_{\mathrm{q.m.}}(r)$ from equation (3), for r varying from 0 to 150 Bohr radii. The sums were terminated when the last term became less than one ten-thousandth part of the sum, and the integral was evaluated using a trapezoidal rule with upper and lower limits, which, when doubled and halved respectively, failed to alter the value of the integral by more than one ten-thousandth of its value.

Figure 1 shows plots of $\log_{10}(g_{\mathrm{q.m.}}(r))$ versus r (Q curves) calculated for three temperatures: 10^4, 2×10^4, and 4×10^4 °K. The curves show that the bound state contribution is quite large, especially at low temperatures, and for 10^4 °K even at 50 Bohr radii the bound states contribute 18% of $g_{\mathrm{q.m.}}(r)$, and still contribute 11% at 100 Bohr radii. The value of n at which the sum of the bound states is terminated is also of interest, and for 10^4°K at 10 Bohr radii 26 terms were needed, at 50 Bohr

radii 84 terms, and at 100 Bohr radii 110 terms contributed. In a similar manner the number of terms contributing to the scattering states increased as the radii increased.

The figure shows that $g_{q.m.}(r)$ runs smoothly onto the classical radial distribution function $g_c(r)$ (C curves) at a certain joining radius r_j, which has been chosen such that the ratio $\{g_{q.m.}(r)-g_c(r)\}/g_c(r)$ is less than 0·05 for $r > r_j$. It can be seen that below r_j there is a marked difference between $g_{q.m.}(r)$ and $g_c(r)$. At $r = 0$ the quantum

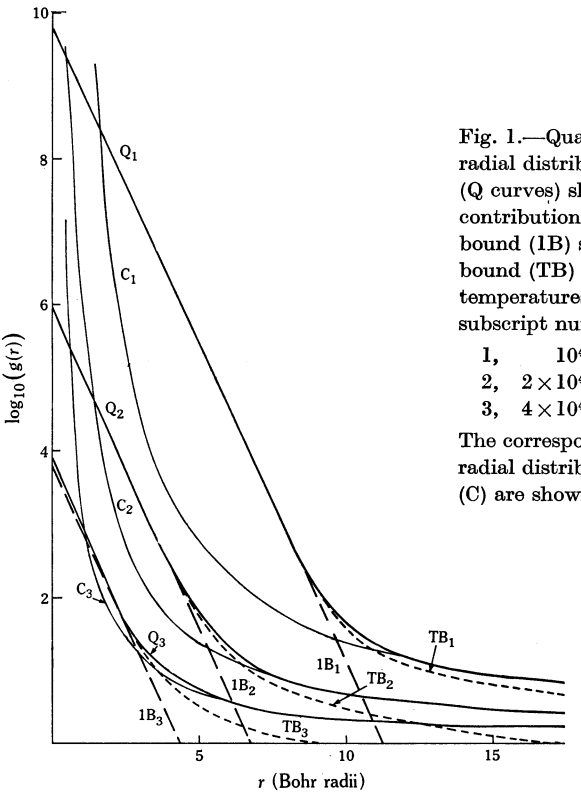

Fig. 1.—Quantum mechanical radial distribution functions (Q curves) showing contributions from the first bound (1B) state and total bound (TB) states for three temperatures indicated by subscript numbers:

1, 10^4 °K,
2, 2×10^4 °K,
3, 4×10^4 °K.

The corresponding classical radial distribution functions (C) are shown for comparison.

mechanical curve tends to a constant (approximately equal to the first bound state contribution of

$$(2\pi\beta\hbar^2/m)^{3/2}\exp(15\cdot780/T\times10^{-4})/\pi$$

for temperatures T below 4×10^4), while the classical curve approaches infinity. For small r and low temperatures the quantum mechanical curve lies close to the first bound state contribution, i.e.

$$(2\pi\beta\hbar^2/m)^{3/2}\exp\{(15\cdot780/T\times10^{-4})-2r\}/\pi$$

(where r is in Bohr radii), whilst the classical curve

$$g_c(r) = \exp\{63\cdot156/(T\times10^{-4}\times2r)\}$$

falls away much more sharply. As the radii increase, other bound states and scattered

states start making an appreciable contribution to $g_{q.m.}(r)$, until at r_j it effectively joins the classical curve.

So far no allowance has been made for the effects of other particles present in the plasma, equation (3) being valid for a two-particle system just as the classical distribution function is valid for a proton–electron system. To take account of this shielding effect is more difficult and, as the procedure is discussed fully in Section IV, it will only be mentioned here that curves are presented below in which an attempt has been made to include the shielding effect approximately.

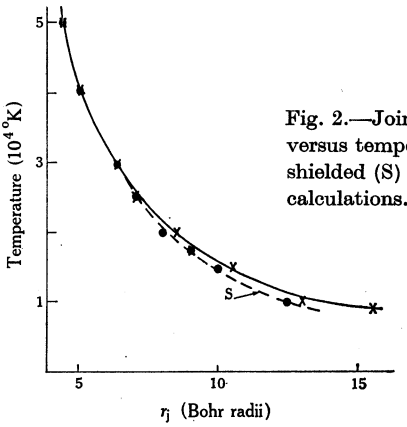

Fig. 2.—Joining radius r_j versus temperature for shielded (S) and nonshielded calculations.

The temperature dependence of the various $g_{q.m.}(r)$ functions is clearly evident from Figure 1. As the temperature is increased the quantum mechanical curve becomes much closer to the classical curve, the bound state contribution falls off much faster, and the contribution of the first bound state is less important. Comparison of $g_{q.m.}(r)$ and the first bound state contribution with recent results obtained by Storer (personal communication), who uses a path integral calculation to obtain $g_{q.m.}(r)$, indicates close agreement with the results presented here. However, Storer's results clearly show that at temperatures above 4×10^4 the first bound state no longer contributes nearly 100% of $g_{q.m.}(r)$ for small radii. In the present results the divergence of $g_{q.m.}(r)$ from the first bound state contribution at $r = 0$ is only just apparent at 4×10^4 °K.

Figure 2 shows that the joining radius r_j falls off sharply as the temperature increases from $0{\cdot}9\times10^4$ to 3×10^4 °K but that at higher temperatures it varies only slightly. There is no obvious analytical dependence of r_j on temperature.

IV. Extension to Allow for Shielding

To include the effects of other particles in the quantum mechanical distribution function to a high degree of accuracy it is necessary to use $g_{q.m.}(r)$ as a first approximation in a modified Percus–Yevick equation, and the author hopes to present results using this approach in the near future. However, in the present paper an

approximate estimate of the shielding effect of other particles is obtained by including a Debye–Hückel shielding factor on the charge of the hydrogen atom, and Z in equation (3) is replaced by $Z\exp(-r/\lambda_D)$, where λ_D is the Debye shielding distance. This involves the approximation that the wavefunctions obtained by solving the Schrödinger equation for a Debye–Hückel shielded potential are equal to the wavefunctions obtained by solving the usual hydrogen atom wave equation, but now weighting these wavefunctions by a Debye–Hückel shielding factor.

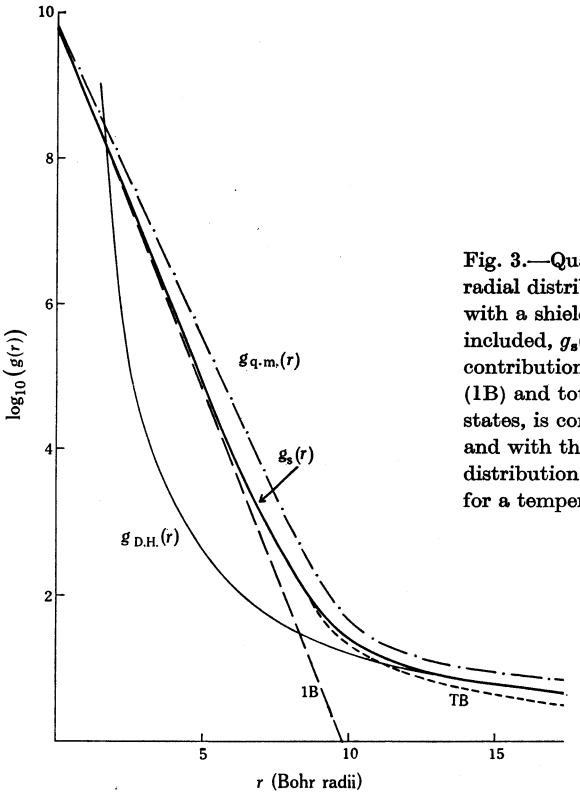

Fig. 3.—Quantum mechanical radial distribution function with a shielding factor included, $g_s(r)$, showing contributions from first bound (1B) and total bound (TB) states, is compared with $g_{q.m.}(r)$ and with the Debye–Hückel distribution function $g_{D.H.}(r)$ for a temperature of 10^4 °K.

Figure 3 shows the radial distribution function including this shielding factor, $g_s(r)$, at 10^4 °K, and comparing it with $g_{q.m.}(r)$ it can be seen that the inclusion of shielding has little effect on the general shape of the curve but lowers it by an appreciable factor, so that now $g_s(r)$ joins the Debye–Hückel curve ($g_{D.H.}(r)$) above a certain radius. From Figure 2 it can be seen that this joining radius (defined as before, except now the criterion is that $g_s(r)$ approaches within 5% of $g_{D.H.}(r)$, not $g_c(r)$ as before) only differs from the nonshielded case at temperatures below 3×10^4 °K. The effect of the shielding is more pronounced on the bound state and first bound state contributions, and Figure 3 shows that these fall off appreciably faster than the nonshielded case.

Figure 4 continues Figure 3 to much higher radii showing that the difference in bound state contribution continues, becoming negligible for the shielded case beyond

the Debye shielding distance λ_D. The classical curve is almost identical to $g_{q.m.}(r)$ and so is not shown, and similarly $g_{D.H.}(r)$ remains so close to $g_s(r)$ that it also is not shown.

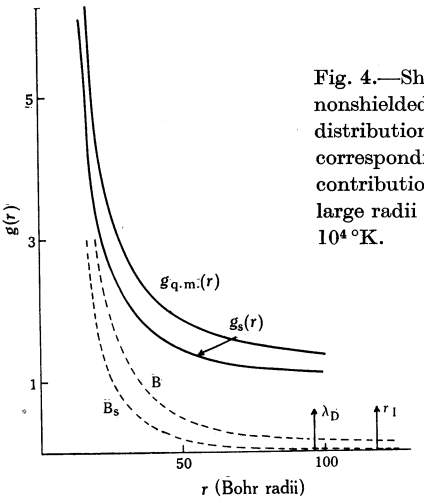

Fig. 4.—Shielded ($g_s(r)$) and nonshielded ($g_{q.m.}(r)$) distribution functions with the corresponding bound state contributions (B_s and B) for large radii at a temperature of 10^4 °K.

V. Ionization

Since the quantum mechanical calculation divides $g_{q.m.}(r)$ into bound and scattered state contributions, it is possible to obtain the percentage ionization present in the hydrogen gas. From the definition of percentage ionization I we have

$$I = \frac{\int_0^{r_I} g_{scatt.}(r)\, 4\pi r^2\, dr}{\int_0^{r_I} g_{q.m.}(r)\, 4\pi r^2\, dr}, \tag{4}$$

where $g_{scatt.}(r)$ is the scattering contribution to $g_{q.m.}(r)$ and r_I is a radius chosen such that $3/4\pi r_I^3$ is the number density (i.e. $4\pi r_I^3/3$ is the volume that on the average contains

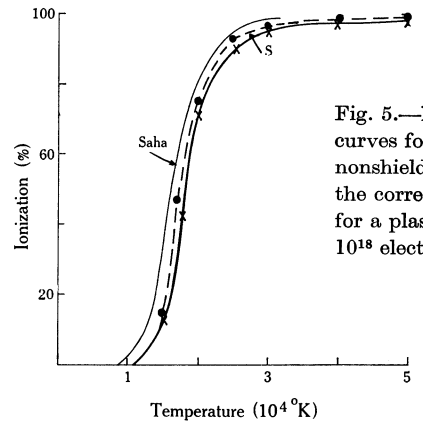

Fig. 5.—Percentage ionization curves for shielded (S) and nonshielded calculations with the corresponding Saha curve for a plasma of density 10^{18} electrons/cm^3.

one electron). Figure 4 shows that r_I is 117·2 Bohr radii for an electron number density of 10^{18} electrons/cm^3, and is larger than the Debye shielding distance.

Figure 5 presents the results of calculations of I by equation (3) using both shielded and nonshielded distribution functions and compares them with Saha's theory (Saha and Saha 1934). The effect of shielding is to increase the ionization some 2 or 3%, which is to be expected, as the shielding precludes some of the bound states. The results agree quite closely with those of Saha, the main disagreement being just above $1{\cdot}5\times10^4\,°\mathrm{K}$, where the nonshielded ionization value is only half the Saha value and even the shielded value is 15% below. Also by Saha's theory, between $1{\cdot}5\times10^4$ and $2\times10^4\,°\mathrm{K}$, 48% of the ionization occurs, while the quantum mechanical calculation gives 59% without shielding and 60% with shielding. At $2{\cdot}5\times10^4\,°\mathrm{K}$ the nonshielded theory implies that there are twice as many neutral particles as the number predicted by Saha's results.

VI. Conclusions

The results are of interest in showing that there are rather large deviations from classical theory at short interparticle distances and that below r_j quantum mechanical effects become important, especially at low temperatures. An approximate allowance for shielding indicates that results are essentially the same for this case, the main difference being in the degree of ionization present. The existing theory in current use is one due to Saha and Saha (1934) and this takes account of the spectrum of bound states in only an approximate way, with no allowance for shielding effects. Nevertheless from the results it can be seen that, by fully taking account of the bound states and also by attempting to allow for shielding, the degree of ionization is surprisingly close to the values obtained by Saha. Also from the results it can be seen that there is some justification in the approach of considering the first bound state as the major contribution to the bound states, especially at temperatures below $3\times10^4\,°\mathrm{K}$ with a density of 10^{18} electrons/cm^3.

VII. Acknowledgments

This work has been carried out with the help of a generous grant from the Australian Institute of Nuclear Science and Engineering for computing. The author wishes to thank Dr. R. G. Storer for informing him of his similar results obtained by a path integral technique. The author is also indebted to Professor H. S. Green for many constructive discussions on the above material and to Dr. P. W. Seymour for helpful advice.

VIII. References

Abramowitz, M., and Stegun, I. A. (1964).—"Handbook of Mathematical Functions." Ch. 14. (National Bureau of Standards: Washington.)

Barker, A. A. (1966).—*Phys. Fluids* **9**, 1590.

Pauling, L., and Wilson, E. B. (1935).—"Introduction to Quantum Mechanics." Ch. V. (McGraw-Hill: New York.)

Saha, M. N., and Saha, N. K. (1934).—"A Treatise in Modern Physics." p. 793. (The Indian Press: Calcutta.)

Schiff, L. I. (1955).—"Quantum Mechanics." Ch. V. (McGraw-Hill: New York.)